Arabidopsis Chloroplastic Glutathione Peroxidases Play a Role in Cross Talk between Photooxidative Stress and Immune Responses[1][W][OA]

Christine C.C. Chang[2,3], Ireneusz Ślesak[2], Lucía Jordá[4], Alexey Sotnikov[5], Michael Melzer, Zbigniew Miszalski, Philip M. Mullineaux, Jane E. Parker, Barbara Karpińska, and Stanisław Karpiński*

Department of Botany, Stockholm University, Frescati 10691 Stockholm, Sweden (C.C.C.C., A.S.); Institute of Plant Physiology, Polish Academy of Sciences, 30–239 Krakow, Poland (I.Ś., Z.M.); Department of Plant-Microbe Interactions, Max-Planck Institute for Plant Breeding Research, D–50829 Cologne, Germany (L.J., J.E.P.); Institute of Plant Genetics and Crop Plant Research, D–06466 Gatersleben, Germany (M.M.); Department of Biological Sciences, University of Essex, Colchester CO4 3SQ, United Kingdom (P.M.M.); and Department of Plants Genetics, Breeding, and Biotechnology, University of Life Sciences, 02–776 Warszawa, Poland (B.K., S.K.)

Glutathione peroxidases (GPXs; EC 1.11.1.9) are key enzymes of the antioxidant network in plants and animals. In order to investigate the role of antioxidant systems in plant chloroplasts, we generated Arabidopsis (*Arabidopsis thaliana*) transgenic lines that are depleted specifically in chloroplastic (cp) forms of *GPX1* and *GPX7*. We show that reduced *cpGPX* expression, either in transgenic lines with lower total *cpGPX* expression (*GPX1* and *GPX7*) or in a *gpx7* insertion mutant, leads to compromised photooxidative stress tolerance but increased basal resistance to virulent bacteria. Depletion of both *GPX1* and *GPX7* expression also caused alterations in leaf cell and chloroplast morphology. Leaf tissues were characterized by shorter and more rounded palisade cells, irregular spongy mesophyll cells, and larger intercellular air spaces compared with the wild type. Chloroplasts had larger and more abundant starch grains than in wild-type and *gpx7* mutant plants. Constitutively reduced *cpGPX* expression also led to higher foliar ascorbic acid, glutathione, and salicylic acid levels in plants exposed to higher light intensities. Our results suggest partially overlapping functions of GPX1 and GPX7. The data further point to specific changes in the chloroplast ascorbate-glutathione cycle due to reduced *cpGPX* expression, initiating reactive oxygen species and salicylic acid pathways that affect leaf development, light acclimation, basal defense, and cell death programs. Thus, cpGPXs regulate cellular photooxidative tolerance and immune responses.

[1] This work was supported by the Polish Science Foundation strategic project Welcome 2008/1 and the Swedish Council for International Cooperation in Research and Higher Education (to S.K.), by a European Union Marie Curie fellowship (grant no. HPMF–CT–2001–01197 to L.J. and J.E.P.) and the Alexander von Humboldt Foundation, by the Institute of Plant Genetics and Crop Plant Research in Gatersleben, Germany (to M.M.), and by the Biotechnology and Biological Sciences Research Council (to P.M.M.).

[2] These authors contributed equally to the article.

[3] Present address: Carnegie Institution of Washington, 260 Panama Street, Stanford, CA 94305.

[4] Present address: Departemento Biotecnología, Centro de Biotecnología y Genómica de Plantas, Campus Montegancedo Universidad Politécnica Madrid, Autopista M40, km38, 28223–Pozuelo de Alarcón, Spain.

[5] Present address: Alexey Sotnikow Institute of Cytology RAS, 4 Tikhoretsky Avenue, 194064 St. Petersburg, Russia.

* Corresponding author; e-mail stanislaw_karpinski@sggw.pl.

The author responsible for the distribution of materials integral to the findings presented in this article in accordance with the policy described in the Instructions for Authors (www.plantphysiol.org) is: Stanisław Karpiński (stanislaw_karpinski@sggw.pl).

[W] The online version of this article contains Web-only data.

[OA] Open Access articles can be viewed online without a subscription.

www.plantphysiol.org/cgi/doi/10.1104/pp.109.135566

Survival under stress depends on the plant's ability to perceive multiple external stimuli and adjust metabolism and growth accordingly (Rao et al., 1997; Shinozaki and Yamaguchi-Shinozaki, 1997). Reactive oxygen species (ROS) such as hydrogen peroxide (H_2O_2), singlet oxygen, and superoxide anion radical ($O_2^{\cdot -}$) are generated during photosynthesis. While enhanced production of ROS can be destructive to cells, ROS also serve as substrates in metabolism and as signaling molecules in acclimation and defense responses (Foyer and Noctor, 2000; Apel and Hirt, 2004). Plant cells have thus evolved effective mechanisms to modulate steady-state levels of ROS inside and also to some extent outside cells (Mittler, 2002). The redox buffers ascorbate and glutathione and associated enzymes (including superoxide dismutases [SODs], catalases [CATs], ascorbate peroxidases [APXs], monodehydroascorbate, glutathione reductases, peroxiredoxins, and glutathione peroxidases [GPXs]) are crucial for such control (Kliebenstein et al., 1998; Asada, 1999; Rey et al., 2007; Ślesak et al., 2007).

In the natural environment, plants normally experience multiple simultaneous stresses. For example,

drought often occurs together with heat, or high light with chilling. These abiotic stresses commonly involve the generation of excess excitation energy (EEE), which arises as a consequence of absorbed light energy being in excess of the amount required to drive compromised photosynthetic metabolism under such conditions (Baker, 2008). Failure to dissipate EEE can result in programmed cell death (Karpinski et al., 1999; Mühlenbock et al., 2008). Such a situation is not necessarily detrimental to the plant, since this can alter responses to pathogens and wounding (Mullineaux et al., 2000; Karpinski et al., 2003; Chang et al., 2004; Mühlenbock et al., 2007, 2008; Ślesak et al., 2007). Accordingly, extensive cross-regulation of pathways governing responses to abiotic and biotic stress stimuli has been observed. For example, responses to biotrophic pathogens, acclimation to conditions that promote EEE, or root hypoxia induce local and systemic reactions resembling those typically observed in response to pathogens (Mateo et al., 2004; Mühlenbock et al., 2007, 2008). Recently, it was demonstrated that systemic acquired resistance (Métraux et al., 1990) and systemic acquired acclimation (Karpinski et al., 1999) share some common metabolic and genetic components (Karpinski et al., 2003; Kiddle et al., 2003; Mateo et al., 2004, 2006; Bechtold et al., 2005; Mühlenbock et al., 2008) and some specific components (Rossel et al., 2007).

GPXs (EC 1.11.1.9) are important ROS scavengers because they have broad substrate specificities and a high affinity for H_2O_2 (Brigelius-Flohé and Flohé, 2003). Their principal activity is thought to catalyze the reduction of H_2O_2 and lipid hydroperoxide to water and alcohol, respectively, using glutathione as the electron donor (Ursini et al., 1995; Fu et al., 2002). In plants, complementary DNAs encoding proteins with significant amino acid homology to animal GPXs have been isolated and characterized. Their roles in ROS homeostasis and stress signaling are unclear (Criqui et al., 1992; Sugimoto and Sakamoto, 1997; Mullineaux et al., 1998; Li et al., 2000; Jung et al., 2002). However, plant *GPX* genes are responsive to abiotic stresses, hormone treatments (Roxas et al., 1997; Avsian-Kretchmer et al., 1999; Milla et al., 2003; Sreenivasulu et al., 2004; Miao et al., 2006), pathogens (Criqui et al., 1992), aluminum toxicity (Milla et al., 2002), and wounding (Depege et al., 1998), and a role for GPXs in limiting an oxidative burst and programmed cell death was reported in Arabidopsis (*Arabidopsis thaliana*; Chen et al., 2004).

In Arabidopsis, *GPX*s are encoded by a gene family of eight members (*AtGPX1* to *AtGPX8*). Based on primary sequence analysis and transit peptide predictions, *AtGPX* family members have been assigned to the cytosol (*AtGPX2*, *AtGPX4*, and *AtGPX6*), chloroplast (*AtGPX1* and *AtGPX7*), mitochondria (*AtGPX3*), and endoplasmic reticulum (*AtGPX5*; Milla et al., 2003). AtGPX8 has not been reported previously and is most likely a cytosolic enzyme, since it lacks a signal peptide (Supplemental Fig. S1, A and B). The different predicted intracellular locations of these GPXs raised the question of whether individual isoforms have particular functions. *GPX1* and *GPX7* mRNAs that were used as expression markers for the induction of resistance against *Pseudomonas syringae* pv *glya* infection (Levine et al., 1994) and encoded enzymes were indeed subsequently shown to be chloroplastic enzymes (Mullineaux et al., 1998). AtGPX1 resides on the thylakoid membrane (Ferro et al., 2003; Peltier et al., 2004) or stroma (Zybailov et al., 2008), while the precise location of AtGPX7 is unclear (Meyer et al., 2005). These two chloroplastic (cp) GPX enzymes have 82% amino acid identity and, therefore, were thought to have overlapping activities (Milla et al., 2003).

We aimed to investigate the contribution of cpAtGPXs to the control of plant stress responses. Here, we have measured the effects of reducing both *AtGPX1* and *AtGPX7* expression as well as the specific loss of *AtGPX7*. Our results suggest that cpGPXs have an important regulatory and protective role during acclimation to photooxidative stress conditions and in limiting programmed cell death in response to infection by virulent and avirulent biotrophic pathogens.

RESULTS

Reduced Expression of *cpGPX*s Compromises Photooxidative Stress Tolerance

To characterize the functions of *AtGPX1* and *AtGPX7*, we generated a series of antisense (AS) transgenic lines in Arabidopsis accession Columbia. Three AS-*cpGPX* lines (denoted 71-90, 71-92, and 71-93) were selected that exhibited reduced expression of both *AtGPX1* and *AtGPX7*, with line 71-93 showing the most depletion (Fig. 1A). A T-DNA insertion mutant of *AtGPX7* (*gpx7*) that was deficient only in *AtGPX7* transcripts was also selected (Fig. 1A). The total GPX activity measured using two substrates, H_2O_2 and *t*-butyl hydroperoxide, in the crude foliar extract was not diminished in AS-*cpGPX* lines 71-90, 71-92, and 71-93 or in the *gpx7* null mutant when compared with wild-type plants (Fig. 1B). However, GPX activity in isolated intact chloroplasts was reduced in the AS lines and the *gpx7* mutant, with AS-*cpGPX* 71-93 exhibiting the strongest reduction (up to 75%) of wild-type chloroplast activity (Fig. 1C). The extent of cpGPX depletion was also evaluated at the protein level using anti-cpGPX antibody (Fig. 1D; Supplemental Fig. S2). In order to produce antibodies against cpGPX, we expressed and purified from *Escherichia coli* a 58-amino acid region between Ser-175 and the C-terminal Ala of GPX7 that is most different from the cytosolic GPX isoforms and has 74% identity to AtGPX1. The anti-cpGPX antibodies recognized an approximately 20-kD band on a western blot corresponding to the size of AtGPX1 and AtGPX7 (Supplemental Fig. S2). Antibodies were purified and tested on western blots of total and chloroplastic protein extracts from wild-type plants and the transgenic 71-90,

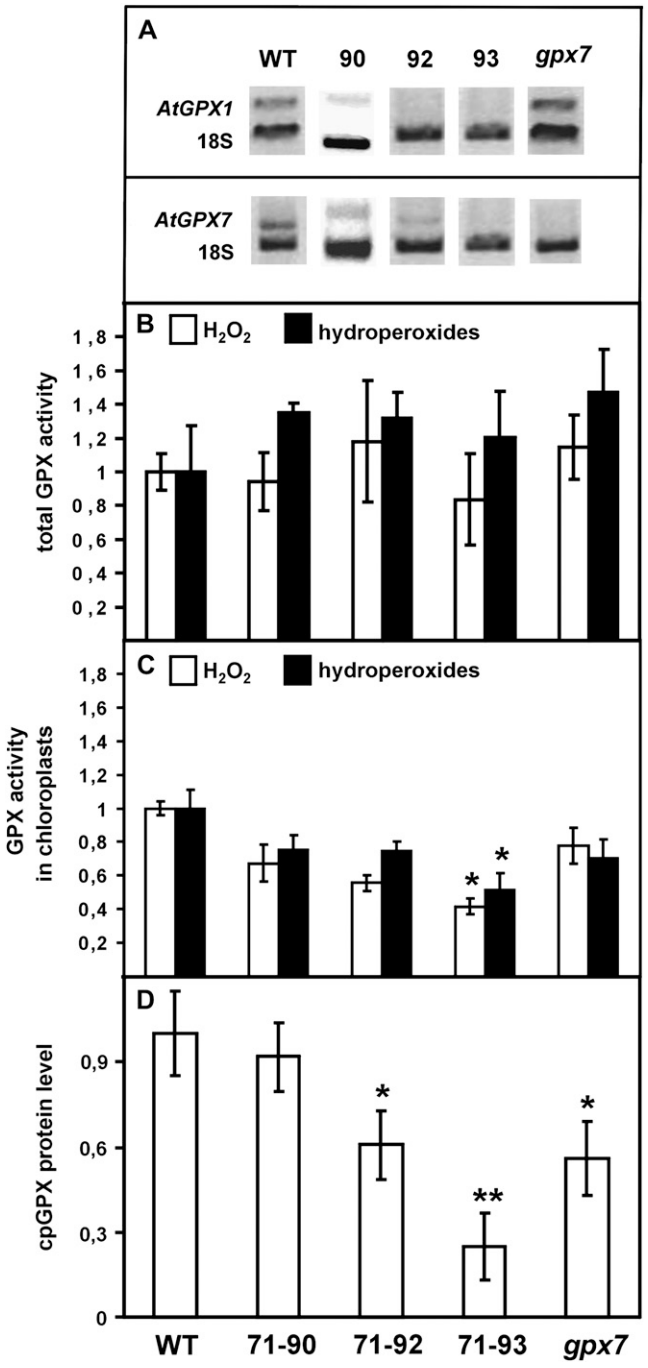

Figure 1. Selected transgenic AS-*cpGPX* lines and *gpx7* have reduced cpGPX activity and protein levels. A, Transcript abundance of *AtGPX1* and *AtGPX7* in selected transgenic Arabidopsis AS-*cpGPX* lines (71-90, 71-92, 71-93, and *gpx7*) measured by reverse transcription-PCR assay using 18S RNA as an internal standard. B, GPX activity measured in crude cell extracts of selected lines. C, GPX activity in extracts of isolated intact chloroplasts. H_2O_2 and *t*-butyl hydroperoxide were used as substrates and expressed as a ratio compared with wild-type (WT) plants. D, cpGPX protein level measured by ELISA and expressed as a ratio to wild-type plants. The values are represented as percentages of control. Mean values (±SD) of six different plants from three independent experiments ($n = 18$) are shown. The asterisks indicate the significance of differences from wild-type plants (* $P < 0.05$, ** $P < 0.01$).

71-92, and 71-93 lines. In an ELISA, amounts of cpGPX from total extracts were reduced by 9%, 40%, 44%, and 75% in AS-*cpGPX* lines 71-90, 71-92, *gpx7*, and 71-93, respectively, relative to wild-type cpGPX protein levels (Fig. 1D). Since these lines were not affected in the expression of other *GPX* family members (Supplemental Fig. S1C), they were considered suitable for analysis specifically of *cpGPX* functions.

Depletion of *cpGPX* expression did not alter rosette size or plant biomass. Regulation of photooxidative and photoinhibitory stress responses and associated acclimation are closely linked and can be monitored by changes in the maximum quantum efficiency of PSII (F_v/F_m). F_v/F_m of the AS-*cpGPX* lines was similar to that of wild-type plants when cultivated under low-light conditions (75 ± 10 μmol m^{-2} s^{-1}; Fig. 2A). It has been shown that induction of several oxidative stress-related genes (including *GPX*s and *SOD*s) occurred only under combined cold/high-light treatments that would cause photooxidative stress (Soitamo et al., 2008). This prompted us to test whether the AS-*cpGPX* lines 71-90, 71-92, and 71-93 or the *gpx7* null mutant were more susceptible to photooxidative stress by combined high light and chilling temperature. When

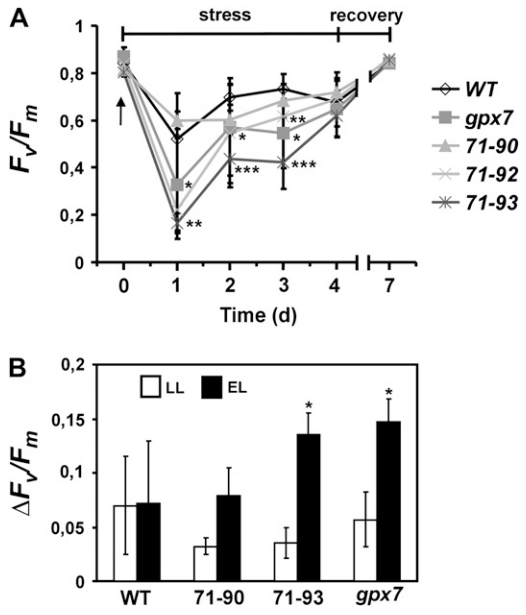

Figure 2. Analysis of photooxidative stress responses in the AS-*cpGPX* lines and the *gpx7* mutant. A, Maximal photochemical efficiency parameter (F_v/F_m) in lines during cold and photooxidative stress (4 d, HLC) and after 3 d in recovery in laboratory growth conditions. Prior to measurements, plants were dark adapted for 30 min. The arrow indicates F_v/F_m initial values for control plants at time 0 growing at 75 ± 10 μmol m^{-2} s^{-1}. B, The difference between F_v/F_m on the leaf abaxial side ($F_v/F_{m[ab]}$) and the adaxial side ($F_v/F_{m[ad]}$) is defined as $\Delta F_v/F_m = F_v/F_{m[ab]} - F_v/F_{m[ad]}$ of LL-acclimated leaves exposed to 1 h of EL. The adaxial and abaxial leaf sides represent palisade and spongy cells in the leaf tissue. Mean values (±SD) of six different plants from three independent experiments ($n = 18$) are shown. The asterisks indicate the significance of differences from wild-type (WT) plants (* $P < 0.05$, ** $P < 0.01$, *** $P < 0.001$).

2-week-old plants were exposed to a combination of high-light stress (650 ± 50 μmol m^{-2} s^{-1}) at chilling temperature (4°C) for 4 d (hereafter called HLC), transient photoinhibition of PSII occurred (Fig. 2A). Reduced F_v/F_m is indicative of photooxidative stress and photoinhibition (Karpinski et al., 1999; Mateo et al., 2004, Baker, 2008). Decreases in F_v/F_m were observed in all plant lines after 1 d of exposure to HLC. However, AS-*cpGPX* lines 71-93 and 71-92 and the *gpx7* mutant displayed a more acute response than the wild type (Fig. 2A). Full recovery in overall F_v/F_m occurred when plants were returned to ambient low light and room temperature conditions for 3 d. The extent of F_v/F_m reduction correlated with cpGPX activities and protein levels in the different lines (Fig. 1, C and D), although all AS-*cpGPX* lines and the *gpx7* mutant were ultimately able to acclimate to changed conditions, as indicated by F_v/F_m levels being similar to those in the wild type at the end of the stress period (Fig. 2A).

Another indicator of leaf susceptibility to the photooxidative stress is the difference in F_v/F_m between the adaxial (directly exposed to the light) and abaxial (not directly exposed to the light) surfaces of the leaves (Lake et al., 2002; Murchie et al., 2005; Driscoll et al., 2006). The difference between F_v/F_m on the leaf abaxial side ($F_v/F_{m[ab]}$) and the adaxial side ($F_v/F_{m[ad]}$) is defined as $\Delta F_v/F_m = F_v/F_{m[ab]} - F_v/F_{m[ad]}$ (Fig. 2B). A substantial $\Delta F_v/F_m$ increase was observed in low light (LL)-acclimated AS-*cpGPX* line 71-93 and *gpx7* compared with the wild type after excess light (EL) for 1 h (Fig. 2B). This result further supports the involvement of cpGPXs in protection of the photosynthetic apparatus and thus the whole plant response to photooxidative stress, with higher photooxidative stress sensitivity on the adaxial side of the leaf in lines with depleted *AtGPX1* and *AtGPX7* expression. These data suggest that plants depleted in *cpGPX* expression are more susceptible to conditions that promote moderate photooxidative stress but nevertheless are able to adjust to such a stress.

This conclusion was further supported by the inhibition of the rate of photosynthetic O_2 evolution (photoinhibition) over a range of photosynthetically active photon flux densities in recovery phase (Fig. 3). Significantly lower photosynthetic O_2 evolution saturation rates were evident in AS-*cpGPX* lines 71-92 and 71-93 (data not shown) and in the *gpx7* mutant grown either in LL or high light (HL; Fig. 3, A and D). For direct comparison, we choose line 71-92 and the *gpx7* mutant, since they have similar reduction of the cpGPX activity (Fig. 1), although they responded in different ways to variable light conditions. After 1 h of exposure to EL (2,000 ± 100 μmol m^{-2} s^{-1}) and a 1-h recovery in LL, the LL-acclimated AS-*cpGPX* 71-92 line and the *gpx7* mutant exhibited similar degrees of photosynthesis inhibition compared with wild-type plants (Fig. 3, B and C). Because the F_v/F_m remained unchanged in LL-acclimated plants (Fig. 2A), this transient decrease in quantum efficiency suggests that cpGPXs play an important role in protecting PSII function during transient increases in excitation energy (in EEE conditions). This was further illustrated in HL-acclimated plants (Fig. 3, E and F), in which inhibition of photosynthesis after EL exposure was significantly different (as indicated by ANOVA and Tukey's posttest) in AS-*cpGPX* line 71-92 compared with the *gpx7* mutant and wild-type plants, even after a 1-h recovery in HL (Fig. 3F). On the other hand, lower oxygen evolution could also result from higher inhibition of the Calvin cycle enzymes due to higher ROS production rates in lines with depleted cpGPX activity under photooxidative stress conditions.

Nevertheless, both the F_v/F_m and oxygen evolution data (Figs. 2 and 3) suggest that sensitivity to and ability to recover from photooxidative stress and photoinhibition are impaired in plants with diminished cpGPX activity. The most affected plants were plants with diminished expression of both *AtGPX1* and *AtGPX7* genes. We reasoned that the capacity for sensing or regulating these stresses must be altered in leaves with reduced cpGPX activities.

Transgenic Lines with Reduced cpGPX Activity Have Higher Foliar H_2O_2 Levels

If depleting cpGPXs in Arabidopsis increases plant sensitivity to photooxidative stress by altering PSII activity, what is the underlying mechanism? The principal biological activity of GPXs is to catalyze the reduction of H_2O_2 and/or lipid hydroperoxides and other organic hydroperoxides (Ursini et al., 1995; Fu et al., 2002). However, we did not observe significant differences in lipid peroxidation between LL-cultivated AS-*cpGPX* and *gpx7* lines and wild-type plants exposed to EL (Fig. 4A). We reasoned that H_2O_2 may be overproduced without any significant change in lipid peroxidation. H_2O_2 content was measured in leaves from plants grown under LL conditions (LL) and LL-acclimated plants after 1 h of EL (LL + EL) using a fluorometric assay. Significantly higher foliar H_2O_2 levels were found in the AS-*cpGPX* lines (71-92 and 71-93) and the *gpx7* mutant after exposure to EL (Fig. 4B). It is notable that basal foliar H_2O_2 levels of the AS-cpGPX lines 71-92 and 71-93 grown under LL were also higher than in wild-type plants and *gpx7* (Fig. 4B). Increased photooxidative stress in the AS-*cpGPX* lines 71-92 and 71-93, but not in 71-90 and the *gpx7* mutant, under HL was associated with a significantly higher accumulation of anthocyanins (Fig. 4C). These results further support our conclusion that depletion of cpGPX leads to increased photooxidative stress.

The intensity, duration, and localization of ROS level changes (such as H_2O_2) require a tight regulatory network (Mittler et al., 2004). In plants, this network includes SODs, CATs, APXs, and GPXs together with other antioxidants for effective cellular ROS homeostasis. We first assessed the effect of GPX depletion on SOD activities, since they are major scavengers of $O_2^{\cdot -}$ and H_2O_2 producers during photooxidative stress.

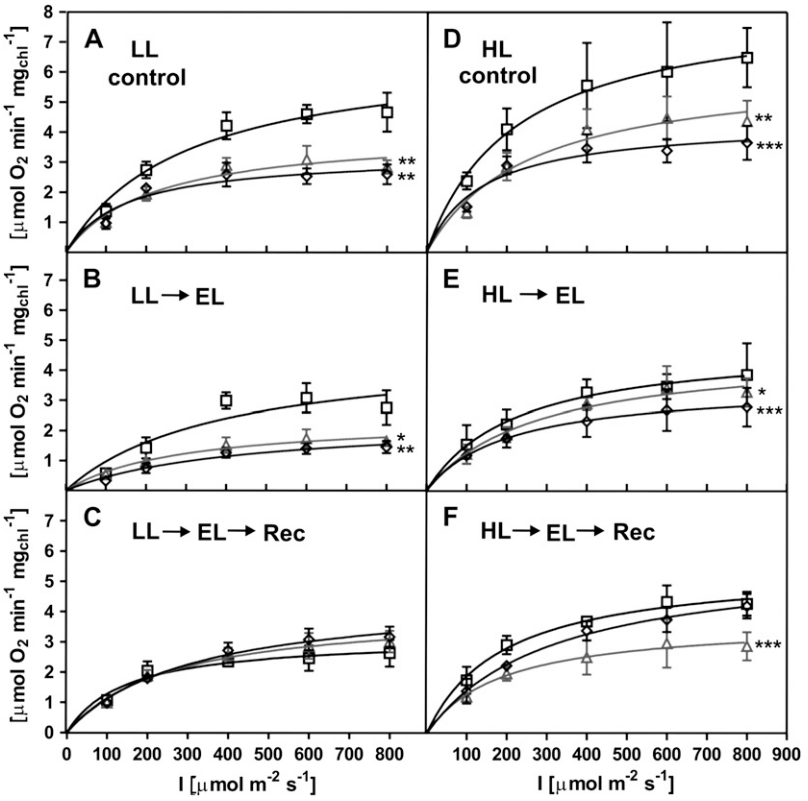

Figure 3. Analysis of photoinhibition in *cpGPX*-depleted lines and wild-type plants. Light response curves for O_2 evolution in the AS-*cpGPX* line 71-92 and *gpx7* mutant leaves grown under different light acclimation conditions (LL, 100 ± 50 μmol m^{-2} s^{-1}; HL, 450 ± 50 μmol m^{-2} s^{-1}). It is important to know that AS-*cpGPX* line 71-92 and the *gpx7* mutant have similar reduction in total cpGPX activity. A and D, Plants acclimated to LL (A) and HL (D). B and E, Plants exposed to EL (2,000 ± 100 μmol m^{-2} s^{-1} for 1 h) after LL acclimation (B) and HL acclimation (E). C and F, Recovery (1 h after EL in LL or HL, respectively) for LL-acclimated plants (C) and HL-acclimated plants (F). Wild-type plants (squares), 71-92 (triangles), and *gpx7* (diamonds) are shown. Values represent means ± SE of pooled samples of three or four leaves from three independent experiments ($n = 3$). Photosynthetic O_2 evolution was measured in a saturating CO_2 atmosphere (0.12%). The asterisks indicate the significance of differences from wild-type plants (mean ± SE; * $P < 0.05$, ** $P < 0.01$, *** $P < 0.001$).

Activity of FeSOD (a chloroplastic form) was not altered in the AS-*cpGPX* lines 71-92 and 71-93 or *gpx7*, whereas activities of cytosolic Cu/ZnSOD I, chloroplastic Cu/ZnSOD II, and mitochondrial MnSOD (Kliebenstein et al., 1998) were reduced in AS-*cpGPX* 71-92 and 71-93 lines (Fig. 4D). In the *gpx7* mutant, we observed a significant reduction only in cytosolic Cu/ZnSOD I and chloroplastic Cu/ZnSOD II (Fig. 4D). The depletion of cpGPXs in AS-*cpGPX* lines and the *gpx7* mutant was not compensated for by higher expression of CAT, which acts as a cytosolic scavenger of H_2O_2 (Supplemental Table S1). However, we observed slightly higher total APX activity in line 71-93 and the *gpx7* mutant, probably caused by induction of the *AtAPX1* gene (Supplemental Table S2).

Leaf and Chloroplast Morphology Is Altered in AS-*cpGPX* and *gpx7* Mutant Plants

Leaf anatomy between the adaxial and abaxial surfaces, consisting of several layers of palisade and spongy mesophyll cells, is highly specialized for light absorption. The increased sensitivity of AS-*cpGPX* 71-92 and 71-93 lines to photooxidative stress led us to hypothesize that leaf morphology becomes adapted to a lower activity of PSII. Light microscopy of leaf sections from LL-acclimated 8-week-old AS-*cpGPX* lines revealed shorter and more rounded palisade cells, irregular spongy mesophyll cells, and larger intercellular air spaces compared with the wild type (Fig. 5, A, C, E, G, and I). The altered morphology was particularly pronounced in AS-*cpGPX* lines 71-92 and 71-93 with larger air spaces (Fig. 5, compare E and G).

We investigated whether there was also a change in chloroplast morphology. Electron microscopy imaging revealed that chloroplasts with reduced cpGPX activity in the AS-*cpGPX* 71-92 and 71-93 lines had larger and more abundant starch grains than in wild-type and *gpx7* mutant plants (Fig. 5, B, D, F, H, and J; samples were taken directly after the dark period). The distribution and number of starch grains in chloroplasts from the AS-*cpGPX* 71-90 line and the *gpx7* mutant were similar to those in the wild type (Fig. 5, compare B and J). By contrast, no differences in the ultrastructure of endoplasmic reticulum, mitochondria, or nucleus were observed among the AS-*cpGPX* 71-90, 71-92, and 71-93 lines, *gpx7* mutant, and wild-type plants (data not shown).

Depletion of cpGPX Reveals Changes in Foliar Levels of Antioxidants and Salicylic Acid

We have shown that the AS-*cpGPX* lines and the *gpx7* mutant have increased sensitivity to transient photooxidative stress (Figs. 2–4). We reasoned that cpGPX depletion likely causes compensatory changes in antioxidant levels in order to cope with the stress; therefore, we measured the accumulation of the major redox buffers ascorbate, glutathione, and salicylic acid (SA). There were no differences in foliar levels of

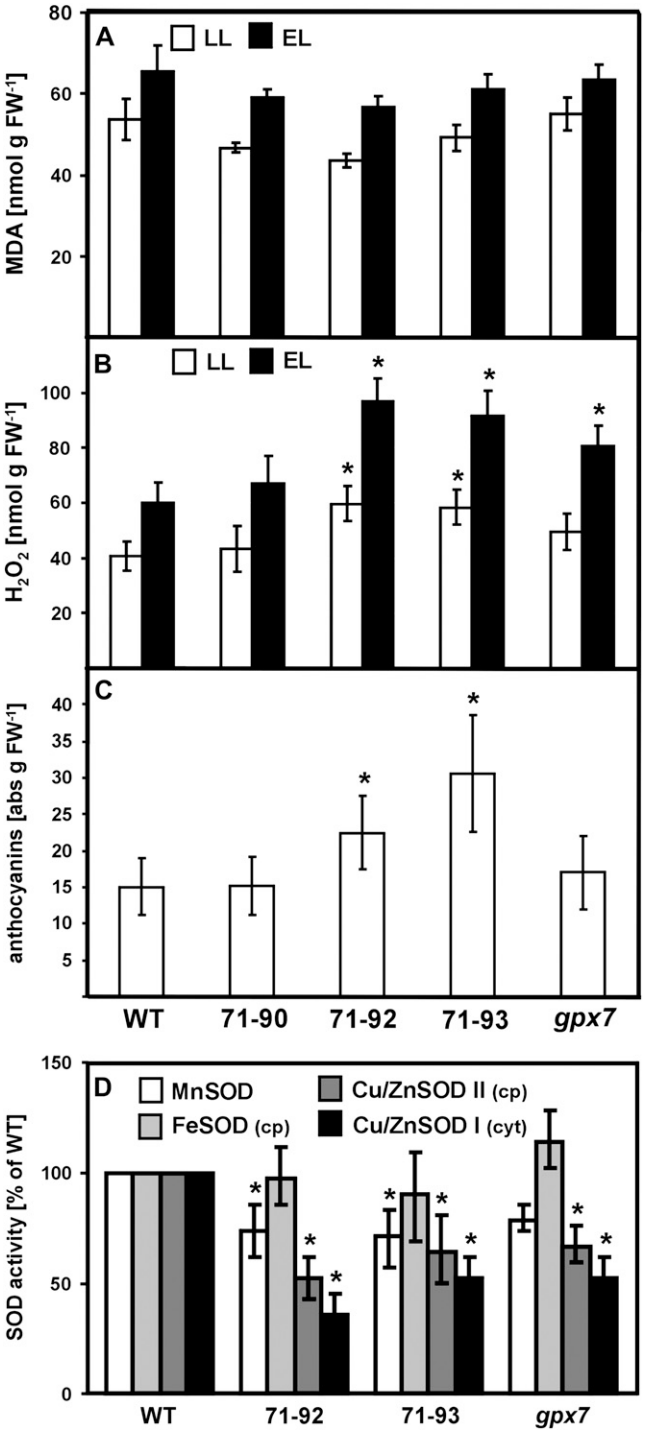

Figure 4. Transgenic lines with reduced cpGPX activity have higher foliar H_2O_2 and anthocyanin levels and reduced SOD activities. A, Quantification of malondialdehyde (MDA) as lipid peroxidation in LL (100 ± 50 μmol m^{-2} s^{-1})-grown plants exposed to 1 h of EL (2,000 ± 100 μmol m^{-2} s^{-1}). B, Quantification of foliar H_2O_2 by a fluorometric assay (Guilbault et al., 1967) from LL-acclimated plants and after 1 h of EL. C, Quantification of anthocyanin content from HL-acclimated plants (450 ± 50 μmol m^{-2} s^{-1}). Mean values (±SD) of pooled leaf samples from three different plants from two or three independent experiments (n = 10–15) are shown. The asterisks indicate the significance of differences from wild-type (WT) plants (* $P < 0.05$). D, Relative activity of four distinct forms of SOD from LL-acclimated plants. Values are expressed in percentages of corresponding SOD activity in wild-type plants (mean ± SD; n = 3; * $P < 0.05$). FW, Fresh weight.

ascorbate, glutathione, and SA in plants cultivated in LL conditions (Table I). However, in plants cultivated in HL, foliar ascorbate, glutathione, and SA levels were significantly higher in AS-*cpGPX* lines 71-92 and 71-93 compared with the wild type. By comparison, only ascorbate levels were higher in *gpx7* mutant leaves under HL conditions (Table I).

R Gene-Triggered Host Cell Death and Basal Defense Responses Are Enhanced in the cpGPX AS Lines

Current evidence suggests a high degree of coregulation of plant responses to abiotic (EEE) and biotic stresses. We investigated whether the *cpGPX* AS lines or the *gpx7* mutant were altered in their response to isolates of the bacterial pathogen *Pseudomonas syringae* pv *tomato* (*Pst*) strain DC3000. Leaves were infiltrated with avirulent *Pst* DC3000 strain expressing *avrRpm1*, and the extent of hypersensitive plant cell death was measured by lactophenol-trypan blue staining. While hypersensitive cell death was restricted to the area around pathogen infection sites in the wild type and the *gpx7* mutant, lesions expanded in the AS-*cpGPX* lines over a period of 72 h after infection (Fig. 6A). We measured the extent of ion leakage as a quantitative indicator of cell death (O'Donnell et al., 2001) by monitoring electrical conductivity of leaf discs 4 d after inoculation with *Pst* DC3000/*avrRpm1*. Similar to the trypan blue staining, the AS-*cpGPX* lines but not *gpx7* displayed more ion leakage than wild-type plants (Fig. 6B). However, growth of *Pst* DC3000/*avrRpm1* was not different in any of the AS plants compared with the wild type. We also measured growth of the virulent strains *Pst* DC3000 (without the *avr* gene) and *Pseudomonas syringae* pv *maculicola* (*Psm*) ES4326. The initial rate of bacterial growth was similar in all tested lines (data not shown). At day 4 after inoculation, however, bacterial titers were at least 10 times lower in the AS-*cpGPX* lines compared with the wild type (Fig. 6C). Therefore, we concluded that depletion of cpGPX activity enhances basal resistance to virulent bacteria.

Meta-Analysis of *AtGPX* Gene Expression Profiles

In order to identify potentially informative expression patterns for particular *GPX*-encoded isoforms, a meta-analysis of *AtGPX* gene expression profiles obtained from publicly available microarray databases (Nottingham Arabidopsis Stock Centre [http://affymetrix.arabidopsis.info/narrays/experimentbrowse.pl] and The Arabidopsis Information Resource [http://www.arabidopsis.org/]) was performed (Supplemental Ta-

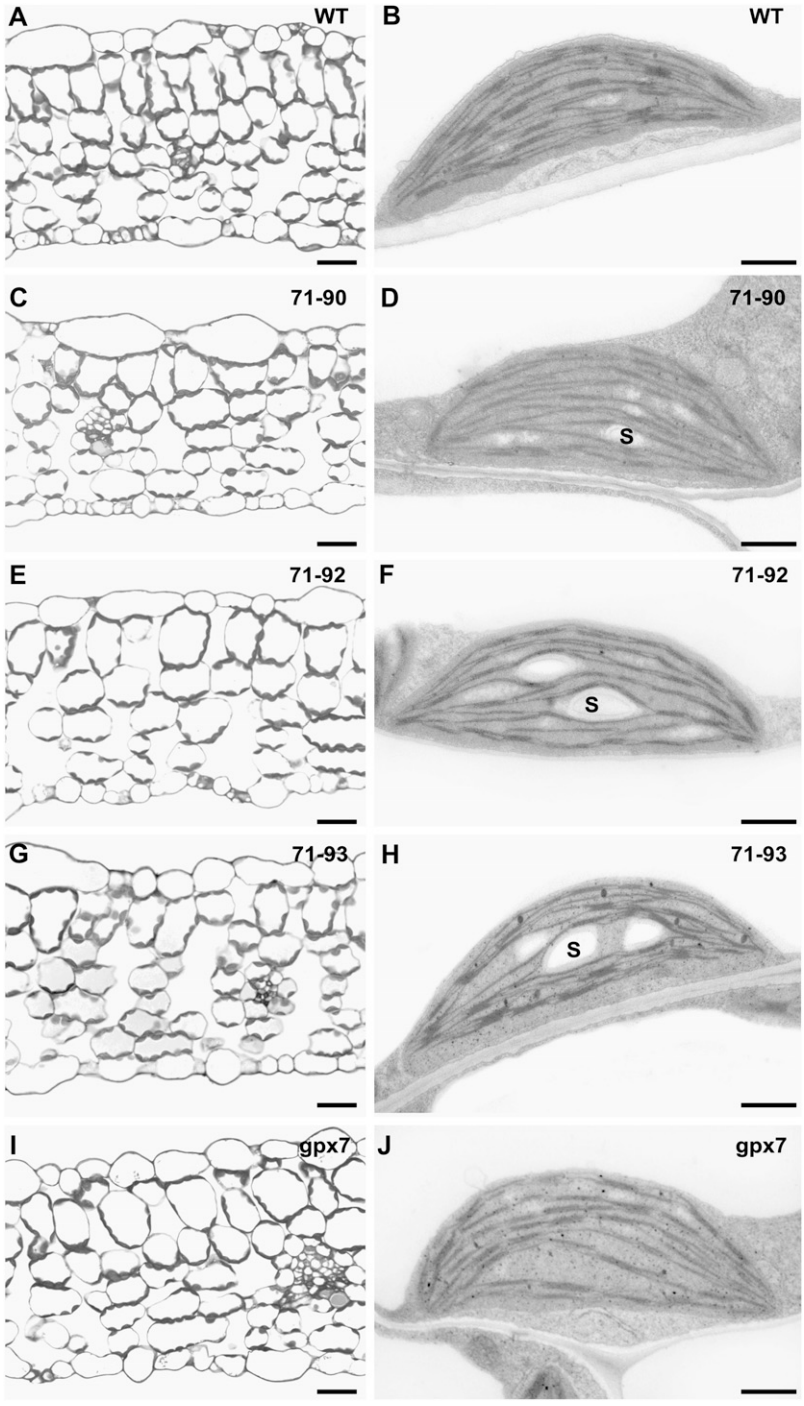

Figure 5. Alterations of leaf and chloroplast morphology of AS-*cpGPX* and *gpx7* lines. A, C, E, G, and I, Leaf section images were obtained from light microscopy of 8-week-old plants with LL acclimation (100 ± 50 μmol m^{-2} s^{-1}): the wild type (WT; A), AS-*cpGPX* lines 71-90 (C), 71-92 (E), and 71-93 (G), and *gpx7* (I). B, D, F, H, and J, Transmission electron microscopy images of chloroplasts from wild-type plants (B), AS-*cpGPX* lines 71-90 (D), 71-92 (F), and 71-93 (H), and *gpx7* (J) with LL acclimation. S, Starch grains. Bars = 25 μm in A, C, E, G, and I and 1 μm in B, D, F, H, and J.

ble S1). We found that *AtGPX1* is responsive to most pathogen treatments (11 of 13 samples tested). Moreover, *cpAtGPX1* expression was suppressed at 2 h after infection with *Pst* DC3000 (no expression changes at 24 h), while *cpAtGPX7* was induced at 24 h after inoculation with the same strain (no expression changes at 2 h). These meta-data support a role of *cpAtGPX1* and *cpGPX7* during pathogen infection and support our and other (Levine et al., 1994) experimental observations.

DISCUSSION

In this study, we aimed to define the role of *AtGPX1* and *AtGPX7* encoding cpGPXs in abiotic and biotic stress responses. Chloroplastic *AtGPX1* and *AtGPX7* have 82% sequence identity and likely have overlapping activities (Supplemental Fig. S1, A and B; Milla et al., 2003), although their responses to different stimuli differ considerably based on meta-analysis of gene expression data (Supplemental Table S1;

Table I. *Foliar levels of conjugated SA, ascorbate, and total glutathione expressed in nanomoles per gram fresh weight of foliar tissue in LL (100 μmol m^{-2} s^{-1})-acclimated and HL (450 ± 50 μmol m^{-2} s^{-1})-acclimated wild-type, AS-cpGPX, and gpx7 mutant plants*

Conjugated SA and total glutathione were measured with HPLC as described by Mateo et al. (2006), and ascorbate was measured spectroscopically as described by Klenell et al. (2005). Results are representative for three independent experiments and pooled samples of three to five leaves from different plants (mean ± SD; $n = 3$). Asterisks indicate significance (*$P < 0.05$, ** $P < 0.01$, *** $P < 0.001$).

Treatment		Wild Type	71-90	71-92	71-93	*gpx7*
Conjugated SA	LL	110 ± 27	122 ± 31	97 ± 23	118 ± 26	121 ± 22
(nmol g^{-1} fresh weight)	HL	168 ± 32	173 ± 35	211 ± 25*	237 ± 38**	202 ± 36
Ascorbate	LL	264 ± 39	302 ± 41	251 ± 36	293 ± 31	307 ± 43
(nmol g^{-1} fresh weight)	HL	483 ± 53	416 ± 48	621 ± 62***	643 ± 61***	568 ± 69*
Glutathione	LL	67 ± 21	85 ± 26	83 ± 17	75 ± 21	91 ± 23
(nmol g^{-1} fresh weight)	HL	141 ± 24	152 ± 35	189 ± 27**	209 ± 31***	167 ± 25

Zimmermann et al., 2004). Thus, GPX1 and GPX7 may have some distinct functions in stress responses. Our results lead us to conclude that *AtGPX1* and *AtGPX7* expression is important for fine-tuning cellular ROS metabolism, photosynthesis, and regulation of light acclimatory and immunodefense responses. Additional unexpected consequences of depletion of *cpGPX* expression were found in leaf mesophyll and chloroplast morphology.

Fine-Tuning of the Photooxidative Stress Tolerance by cpGPXs

Depletion of *AtGPX1* and *AtGPX7* expression compromises the plant's ability to tolerate acute photooxidative stress (Figs. 2–4; Table I). Notably, *AtGPX7* was not fully redundant with *AtGPX1*, reinforcing the notion that there may be a degree of functional specificity between particular chloroplast GPX enzymes. Importantly, we found that increased acute sensitivity to such a stress is proportional to the extent of *AtGPX1* and *AtGPX7* depletion. Our results suggest that cpGPXs help to regulate photooxidative stress tolerance and are important for optimization of the photosynthetic apparatus performance in conditions that promote EEE, such as chilling temperature combined with HL or EL alone (Soitamo et al., 2008). In addition, different photoinhibitory reactions of wild-type plants and transgenic or mutated lines acclimated to LL or HL and then exposed to EL support the idea of some distinct roles of GPX1 and GPX7 in protection of PSII activity, Calvin cycle activity, and chloroplast-nucleus retrograde signaling (Figs. 2–5).

Lipid peroxidation is a major indicator of oxidative damage in cells and is a marker for membrane perturbation and inactivation of membrane proteins leading ultimately to cell death (Avery and Avery, 2001). We did not observe significant differences in lipid peroxidation among AS-*cpGPX* lines, the *gpx7* mutant, and wild-type plants under EL stress (Fig. 4A). Also HL-acclimated leaves of the ascorbate-deficient Arabidopsis mutant *vitamin C defective2* did not exhibit higher levels of lipid peroxidation (Müller-Moulé et al., 2004). These data suggest that cpGPXs predominantly control ROS levels in the hydrophilic phase of the chloroplasts. This was reflected by significantly higher H_2O_2 levels in both LL-acclimated and EL-exposed AS-*cpGPX* lines 71-92 and 71-93 compared with wild-type plants (Fig. 4B), increased foliar levels of anthocyanins (Fig. 4C), depleted Cu/ZnSOD and MnSOD activities (Fig. 4D), and slightly induced *APX1* gene expression (Supplemental Table S2). Thus, lowered cpGPX activity is associated with higher foliar H_2O_2, possibly of chloroplast origin, and the results support close cooperation between cpGPXs and Cu/ZnSODs in the ascorbate-glutathione (water-water) cycle (Asada, 1999; Foyer and Noctor, 2000).

Fine-Tuning of Chloroplast Signaling and Regulation of Leaf Morphology by cpGPXs

Accumulation of H_2O_2 in leaves of CAT-deficient tobacco (*Nicotiana tabacum*) plants was sufficient to induce cpGPX (Chamnongpol et al., 1998). Higher lipid peroxidation was also observed in CAT-deficient mutants and transgenic plants with reduced CAT activity (Montillet et al., 2005). In our transgenic AS-cpGPX and *gpx7* mutant plants, we did not observe enhanced CAT activities (Supplemental Table S2), suggesting that chloroplastic and peroxisomal signaling might have certain distinct regulatory properties. This is supported by the observation of higher foliar ascorbate, glutathione, and SA levels (the last two predominantly synthesized in the chloroplast; Wildermuth et al., 2001; Ball et al., 2004) with correlated reduced chloroplastic and cytosolic Cu/ZnSOD and mitochondrial Mn-SOD activities in the AS-*cpGPX* lines and chloroplastic and cytosolic Cu/ZnSOD activity in the *gpx7* mutant (Fig. 4D). Reduction of SOD activities was inversely proportional to foliar levels of H_2O_2 and anthocyanins (Fig. 4) and is consistent with cpGPXs working together with SODs in the regulation of $O_2^{\cdot -}$ and H_2O_2 cell/chloroplast homeostasis. Higher H_2O_2 levels inhibit Cu/ZnSOD and FeSOD activities (Asada et al., 1975; Alscher et al., 2002). The observed reduction in Cu/ZnSOD activity might be explained by the higher accumulation of H_2O_2 detected in transgenic lines and *gpx7* (Fig. 4D). However, this would not

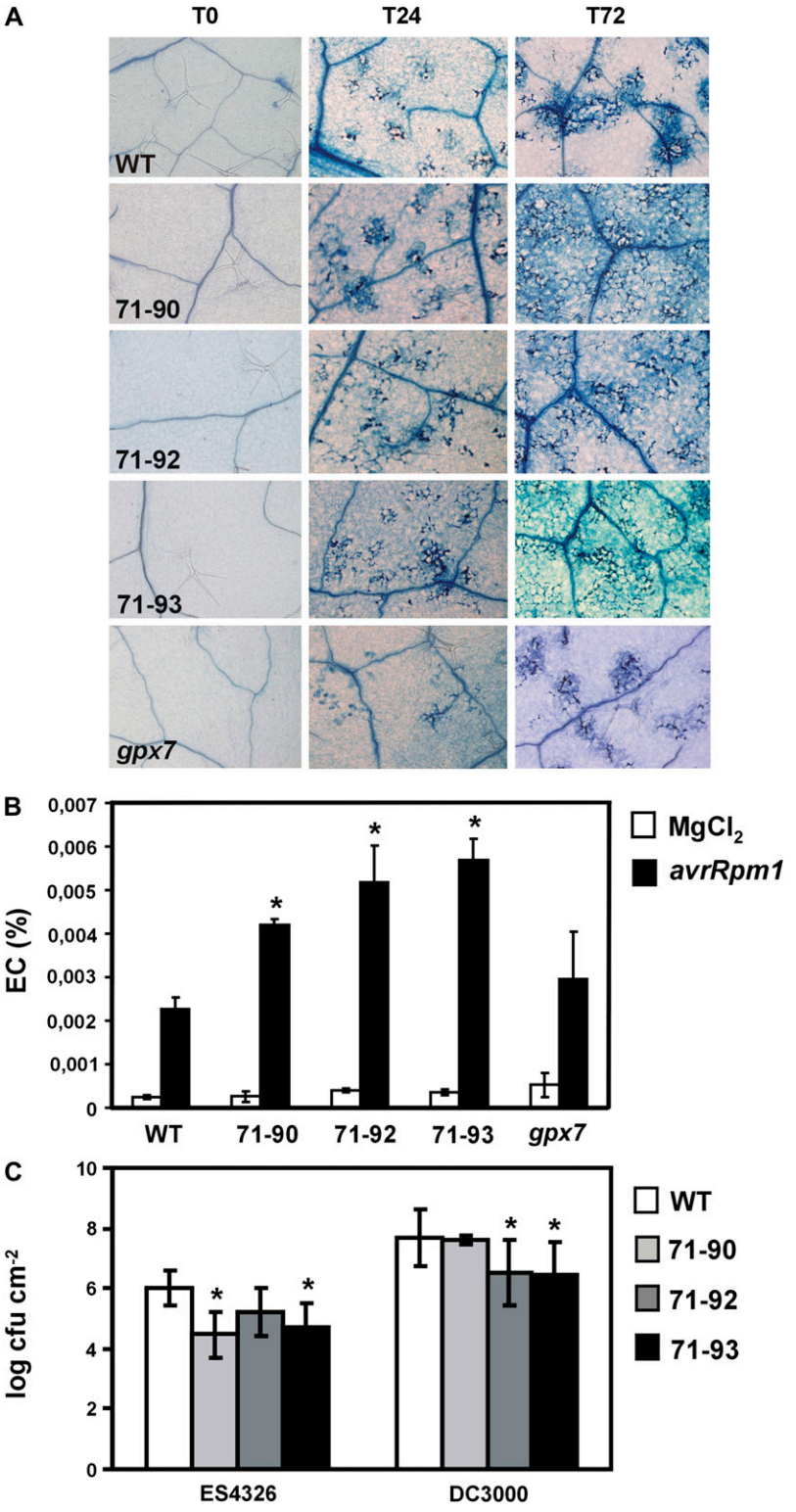

Figure 6. Transgenic lines with reduced *cpGPX* expression displayed enhanced cell death and resistance to *Pseudomonas* bacteria. LL (100 ± 50 μmol m^{-2} s^{-1})-acclimated leaves of 4-week-old plants were infiltrated with a bacterial suspension containing 10^5 colony-forming units (cfu) mL^{-1} in 10 mM $MgCl_2$. A, Trypan blue staining was done at 0 (T0), 24 (T24), and 72 (T72) h after inoculation with avirulent *Pst* DC3000 expressing *avrRpm1*. B, Electrical conductivity (EC) was measured 4 d after infiltration of leaves with *Pst* DC3000/*avrRpm1* or with 10 mM $MgCl_2$ (as a nonspecific wound control). C, Bacterial growth at 4 d after inoculation of virulent strains *Psm* ES4326 and *Pst* DC3000. Mean values ± SD of $n = 45$ are shown. Results were obtained from three independent experiments. Asterisks indicate significant differences from wild-type (WT) plants at $P < 0.05$.

explain effects on MnSOD, which is generally more resistant toward higher H_2O_2 and predominantly located in mitochondria (Dutilleul et al., 2003). On the other hand, no significant reduction of FeSOD activity was observed in AS-*cpGPX* lines and *gpx7* mutant plants showing higher than wild-type accumulation of foliar H_2O_2 (Fig. 4, B and D). This could be due to the fact that FeSOD in Arabidopsis is more resistant to H_2O_2 than Cu/ZnSODs. Alternatively, this result leads us to speculate that *FeSOD* gene regulation in plants

with deregulated expression of *cpGPX*s is altered compared with that in wild-type plants.

Anthocyanins act as a powerful antioxidant that helps protect plants from ROS damage (Teng et al., 2005). The higher anthocyanin levels in AS-*cpGPX* lines under HL conditions (Fig. 4C) are consistent with a further metabolic link between cpGPX activity and anthocyanin synthesis, reinforcing earlier observations (Vanderauwera et al., 2005). Thus, plants with reduced *AtGPX1* and *AtGPX7* expression are more susceptible to moderate photooxidative stress, and these genes play a specific role in protection of the photosynthetic apparatus and regulation of chloroplastic and mitochondrial ROS homeostasis during EEE conditions. By contrast, Rey et al. (2007) demonstrated that compromised H_2O_2 scavenging in the chloroplast, as a result of inhibition of expression of a gene encoding chloroplastic sulfiredoxin, leads to an increased tolerance to moderate photooxidative stress, probably because of compensatory changes in other antioxidant defenses (Rey et al., 2007). This suggests that the opposite situation results from what appears to be a similar disruption of H_2O_2 homeostasis in the chloroplast, reflecting the complexity of the ROS scavenging system and redox homeostasis in the chloroplast.

Chloroplast and mitochondrial homeostasis and retrograde chloroplast-to-nucleus signaling have been shown to control light acclimatory and defense responses (Kiddle et al., 2003; Ball et al., 2004; Mateo et al., 2004, 2006; Mühlenbock et al., 2007, 2008). Our results also suggest that cpGPX activity could be somehow coupled with Cu/ZnSOD and MnSOD activities, for example, through feedback mechanisms that control chloroplastic and mitochondrial ROS homeostasis and, in consequence, photooxidative stress responses (Fig. 4; Table I). Nevertheless, more experimental data are needed to conclude the presence or absence of such a putative feedback mechanism.

Significantly, we found that the adaxial side of a leaf is more prone to photooxidative stress than the abaxial side in the AS-71-93 transgenic line and *gpx7* mutant plants (Fig. 2B). This correlates with anatomical changes in the shape of spongy mesophyll cells and the size of air spaces through which CO_2 and O_2 circulate as well as with starch grain size in chloroplasts (Fig. 2, A, C, E, G, and I) in 71-93 but not in *gpx7* plants. To our knowledge, such morphological traits have not been shown to be associated with cpGPX activities. These observations reinforce the idea that AtGPX1 and AtGPX7 may have distinct functions, since such traits were not observed in the *gpx7* mutant. Moreover, it suggest that *AtGPX1* and *AtGPX7* expression may be particularly important during natural photooxidative stress in plants growing, for example, in springtime in a temperate climate when reflected sunlight, such as from snow, induces additional stress on the abaxial side of a leaf (Karpinski et al., 1993). Chloroplasts of AS-*cpGPX* lines, but not the *gpx7* mutant, have more starch grains (Fig. 5, B, D, F, H, and J), which could be due to altered redox status of the photosynthetic electron carriers and chloroplast sugar metabolism, especially recycled soluble sugars during photosynthesis. Soluble sugars have been implicated in the regulation of ROS-producing/scavenging metabolic pathways, and this is supported by our previous observation that many different DNA cis-regulatory elements, including those in *GPX1* and *GPX7* promoter sequences, have dual functions in ROS and Suc signaling (Geisler et al., 2006). These results suggest that cpGPX activity is required for optimization of chloroplast and cellular metabolism under conditions that promote EEE.

Fine-Tuning of the Immunodefenses by cpGPXs

The phenylpropanoid pathway generates complex secondary metabolites such as flavonoids and isoflavonoids (Dixon et al., 2002). Anthocyanins and benzoic acids also derive from phenylpropanoids. The C_6C_1 benzoic acids include SA as an important defense signal (Winkel, 2004; Strawn et al., 2007). Increased levels of SA were detected in the AS-*cpGPX* 71-92 and 71-93 lines compared with wild-type plants, correlating with higher foliar ascorbate and glutathione levels (Table I) and enhanced disease resistance (Fig. 6). It may be significant that the highest levels of SA, glutathione, and ascorbate (Table I) were observed in AS-*cpGPX* line 71-93, which consistently displayed the highest basal resistance to virulent *Pst* DC3000 and *Psm* ES4326 bacteria (Fig. 6). The enhanced resistance may be associated with specific redox changes of the plastoquinone pool (Karpinski et al., 1999; Mühlenbock et al., 2008) and subsequent activation of the phenylpropanoid pathway and its related products under EEE conditions (Table I; Mateo et al., 2006).

Ascorbate and glutathione play an essential role in chloroplastic protection against the potentially deleterious effects of ROS, acting as direct antioxidants and fulfilling other functions related to redox sensing and signaling (Wingsle and Karpinski, 1996; Karpinski et al., 1997, 1999; Karpinska et al., 2000; Kiddle et al., 2003; Mateo et al., 2006). Recently, we demonstrated that glutathione and SA signaling are functionally integrated (genetically and physiologically) in acclimation to conditions that promote EEE and in plant immune responses (Mateo et al., 2004, 2006; Mühlenbock et al., 2007, 2008). Moreover, retrograde chloroplast-to-nucleus signaling in response to conditions that evoke EEE in Arabidopsis is regulated by *LESION SIMULATING DISEASE1*, *PHYTOALEXIN DEFICIENT4*, *ENHANCED DISEASE SUSCEPTIBILITY1*, and *ETHYLENE INSENSITIVE2* (Mateo et al., 2004; Mühlenbock et al., 2007, 2008). The results presented here point to an important role of cpGPXs in chloroplastic ROS homeostasis and redox signaling between cellular compartments that may coordinate acclimatory and defense responses. Probably, plants have evolved defense mechanisms that depend on light acclimatory responses and retrograde chloroplast sig-

naling that are likely to be crucial to Darwinian fitness in the natural environment, where acclimation to prevailing stresses needs to be integrated. Rapid changes in light intensity and quality, humidity, and temperature make acclimation to the natural environment an imperative.

MATERIALS AND METHODS

Plant Material

Arabidopsis (*Arabidopsis thaliana*) plants were germinated and grown in conventional soil (Topstar-Economa Garden) with a thin layer of autoclaved clay for 4 to 5 weeks under controlled environmental conditions: 9-h/15-h photoperiod at 22°C in a relative humidity of 50% to 60% (LL of 100 ± 50 μmol m^{-2} s^{-1} or HL of 450 ± 50 μmol m^{-2} s^{-1} at 22°C). In all experiments, unless otherwise stated, the accession Columbia was used. All mutants used in this study were obtained from the Nottingham Arabidopsis Stock Centre.

EL conditions were described previously (Karpinski et al., 1999). For high light and cold stress (denoted as HLC), 2-week-old seedlings from a long-day chamber (75 ± 10 μmol m^{-2} s^{-1} during a 16-h/8-h photoperiod in a relative humidity of 50%–60%) were transferred to continuous high light (650 ± 50 μmol m^{-2} s^{-1}) at 4°C for 4 d. At day 4, plants were returned to the initial growth conditions and analyzed after 3 d of recovery (called the "recovery period"). The measurements of F_v/F_m were done using six technical repeats on six leaves from each line of plants during the HLC and the recovery period in the initial growth conditions. Three independent experiments were performed.

AS Constructs and Selection of Transgenic Plants

The cDNA clone (181O9T7) encoding chloroplast GPX (*AtGPX1*) in pBluescript SKII+ (Alting-Mees and Short, 1989) was ordered from the European Molecular Biology Laboratory (http://www.ebi.ac.uk/embl/). A cDNA clone was used to amplify the 500-bp PCR fragments carrying *Hin*dIII and *Eco*RI restriction sites from the 3′ nonconserved part of the genes (forward, 5′-CGTACGGATCCTTCTCTACAGTCCG-3′; reverse, 5′-GGTCCATTCAC-GTCAACCTTATCA-3′). The fragment was cloned in the AS orientation in the vector pJIT60 (Guerineau and Mullineaux, 1993) between the double cauliflower mosaic virus 35S promoter and the cauliflower mosaic virus 35S terminator. The whole 35S cassettes were subsequently cut out using *Sst*I and *Xho*I and inserted between *Sst*I and *Sal*I restriction sites of pBIN19 binary vector (Bevan, 1984). *Agrobacterium tumefaciens* strain GV3101 was used for transformation. The integrity of the construct was verified by sequencing after isolation from *Agrobacterium* and amplification in *Escherichia coli*.

Twelve primary transformant lines were isolated and self-pollinated. About 200 plants from the T2 generation for each line were analyzed for kanamycin resistance. Lines segregating with a ratio of 3:1 were kept, and the T4 generation was obtained for identification of homozygous lines. Selected lines were back-crossed to wild-type plants, and homozygous transgenic lines were selected to create comparable genetic backgrounds. Finally, three transgenic AS-*cpGPX* lines (71-90, 71-92, and 71-93) and one transgenic knockout of *AtGPX7* (*gpx7*) obtained from the Sainsbury Laboratory Arabidopsis Transposants population but genetically cleaned up in our laboratory and later compiled into an Arabidopsis database (Tissier et al., 1999) were chosen for further experiments.

Isolation of Chloroplasts

Intact chloroplasts were isolated from Arabidopsis leaves according to Weigel and Glazebrook (2002). The leaves were homogenized with a blender in precooled medium containing 50 mM HEPES (pH 7.5), 0.33 M sorbitol, 2 mM EDTA, and 1 mM $MgCl_2$. The homogenate was squeezed through two layers of Miracloth (Calbiochem) and cheesecloth (SelefaTrade), and the filtrate was centrifuged at 1,300*g* for 8 min. The pellets were resuspended in the same medium and loaded onto a two-step density gradient with 40% and 80% Percoll (Sigma-Aldrich). After centrifugation at 3,750*g* for 8 min, the intact chloroplast layer between the 40% and 80% Percoll fractions was collected and verified with a microscope.

cpGPX Antibody Production and ELISA

In order to produce antibodies against cpGPX, a 58-amino acid region between Ser-175 and the C-terminal Ala of *AtGPX7*, which is the most different from the cytosolic form of GPXs, was chosen (Supplemental Fig. S1). This sequence has been expressed in fusion with thioredoxin protein and His-Tag using the pET32a vector (Novagen) in *E. coli* BL21DE3 strain. For purification of the fusion protein, we used the Chelating Sepharose Fast Flow (Amersham Biosciences) charged with nickel ions. Purified protein was loaded on a preparative polyacrylamide gel, visualized by Pierce Gel Code staining (Pierce), and then cut out from the gel and used to immunize two rabbits. Immunization of rabbits was conducted by Agrisera on a commercial base. Obtained sera were purified and tested in western blot experiments on total and chloroplastic protein extracts from wild-type plants and transgenic Arabidopsis lines. Both sera gave specific signals of expected molecular mass of approximately 20 kD in the crude protein extract.

For further quantification of cpGPX protein levels in Arabidopsis, ELISA with modification (Mett et al., 2000) was used. The samples, previously quantified using the Bradford assay to ensure equal loading, were transferred to 96-well polystyrene microtiter plates (Nunc-Immuno-Plate, Maxisorb; Nunc) at room temperature for 1 h with shaking. After adding blocking solution (0.5% in phosphate-buffered saline + 0.1% Tween), primary antibodies, secondary antibody, and the color substrate *ortho*-phenylenediamine (Sigma-Aldrich), the reaction was stopped after 15 min of incubation by the addition of 50 μL of 5 M sulfuric acid. The optical density was determined at 450 nm on a microplate reader (Bio-Tek Instruments). A pool of samples from six plants for each line was collected, five technical repeats were measured, and three independent experiments were performed.

GPX Activity

GPX activity was assayed spectrophotometrically according to Drotar et al. (1985) with H_2O_2 or *t*-butyl hydroperoxide as substrate. The rate of peroxide removal was measured with respect to the rate of NADPH oxidation at 348 nm. A pool of samples from six plants for each line was collected, six technical repeats were measured, and three independent experiments were performed.

Chlorophyll Fluorescence and Oxygen Evolution Measurements

The fast chlorophyll *a* induction kinetics were measured as described previously (Karpinski et al., 1999) using an FMS1 portable modulating fluorimeter, the manufacturer's software (Hansatech Instruments), and a protocol similar to that described by Genty et al. (1989). The chlorophyll *a* fluorescence parameter F_v/F_m was calculated according to Maxwell and Johnson (2000). Six leaves were used for each time point, and three independent experiments were done. Oxygen-exchange rates were measured in several leaves in gas phase with saturated CO_2 (0.12%) using a Clark-type oxygen electrode (LD2/3 oxygen electrode chamber) connected to an Oxylab control unit (Hansatech Instruments) and recorded online with a computer using Hansatech software.

Preparation of RNA and Quantitative Reverse Transcription-PCR

Harvested leaf tissue or other specified parts of the plant were frozen and ground to a fine powder in liquid nitrogen. RNA extraction was performed using a Qiagen RNeasy plant mini kit (Qiagen) followed by a DNA-free kit (Ambion). The first cDNA strand was synthesized with the RETROscript kit (Ambion). PCRs were performed using specific primers custom made by Invitrogen and combined with 18S RNA as an internal standard (QuantumRNA 18S; Ambion). The accession numbers for the *GPX* family in Arabidopsis are as follows: *AtGPX1* (At2g25080), *AtGPX2* (At2g31570), *AtGPX3* (At2g43350), *AtGPX4* (At2g48150), *AtGPX5* (At3g63080), *AtGPX6* (At4g11600), *AtGPX7* (At4g31870), and A*tGPX8* (At1g63460). A pool of samples from three plants for each line was collected, and two independent experiments were performed.

Pathogen Assays

Pseudomonas syringae strains were cultured and prepared for inoculations as described previously (Bartsch et al., 2006). Bacterial dilutions in 10 mM

$MgCl_2$ were inoculated into the underside of intact leaves of 4-week-old Arabidopsis plants using a syringe without needle. To determine bacterial growth in leaves, leaf discs (1 cm^2) were harvested and bacteria were extracted by macerating discs with a plastic pestle in 0.3 mL of 10 mM $MgCl_2$. Serial dilutions were plated on peptone-yeast extract-glycerol medium plates containing selective antibiotics. Bacterial titers were determined at 0 and 4 d after inoculation. Three leaf discs were taken per plant, and five plants were used for each line and time point. Three independent experiments were performed.

Cell Death Measurements

Development of the hypersensitive cell death response in leaf tissues was monitored by staining with lactophenol-trypan blue and destaining in saturated chloral hydrate as described (Koch and Slusarenko, 1990). Samples were mounted on slides in 60% glycerol and examined using a light microscope. Cell death was quantified by cellular electrolyte leakage from rosette leaves as described by Overmyer and colleagues (2000). Conductivity was determined after incubating three leaves for 1 h in 5 mL of distilled water with an inoLab Cond Level 1 conductivity meter (Wissenschaftlich-Technische Werkstätten GmbH). Three samples were taken per time point from three different plants for each line, and three independent experiments were performed.

H_2O_2 Quantifications

Quantification of H_2O_2 was performed by a fluorometric assay accordingly to the method described by Guilbault et al. (1967). Approximately 100 mg of leaf material was collected and immediately frozen in liquid nitrogen. The extraction was carried out on ice in 1 mL of extraction medium (50 mM HEPES, pH 7.5, 1 mM EDTA, and 5 mM $MgCl_2$). The homogenized tissue was centrifuged for 10 min at 21,000*g* and 4°C. Supernatant was mixed (1:1) and vortexed for 30 s with a chloroform:methanol mixture (2:1). Afterward, the mixture was centrifuged for 10 min at 11,000*g*, and the water phase was collected. This procedure was repeated twice. A total of 400 μL of the water phase was mixed with 2.6 mL of reaction mixture (50 mM HEPES, pH 7.5, 0.5 μM homovanilic acid, and 4 μM horseradish peroxidase) in a fluorometric cuvette and incubated for 10 min. The measurement of H_2O_2 was made in a Hitachi F2500 fluorometer at 315 nm and 425 nm for excitation and emission, respectively. A standard line was made using 0 to 33 nmol mL^{-1} H_2O_2. The values were calculated in nmol g^{-1} fresh weight. Two independent experiments were performed.

Lipid Peroxidation Quantifications

Malondialdehyde was determined using Bioxytech kit LPO-586 following the manufacturer's instructions. A pool of leaves from three different plants for each line was taken, five technical repeats were measured, and three independent experiments were performed.

Anthocyanin Quantification

Anthocyanin extraction and spectrophotometric quantification were performed as described by Noh and Spalding (1998). The amount of anthocyanin is presented as the values of $A_{535} - 2(A_{650})$ per gram fresh weight. A pool of leaves from three different plants for each line was taken, five technical repeats were measured, and two independent experiments were performed.

Preparation of Soluble Proteins, Native PAGE, Staining, and Evaluation of SOD Activity

To isolate fractions of soluble proteins, two to three frozen leaves were homogenized in 150 μL of the medium (100 mM Tricine, adjusted with Tris to pH 8, 3 mM $MgSO_4$, 1 mM dithiothreitol, and 3 mM EDTA). Nonsoluble material was removed by centrifugation for 1 min at 10,000*g*. Native PAGE was performed at 4°C and 180 V on 12% polyacrylamide gels according to Miszalski et al. (1998). For each lane, 10 or 5 μg of protein extract was applied. Protein concentration was determined according to Bradford (1976) using the Bio-Rad protein assay kit with bovine serum albumin as the standard. Activity of SOD on the gels was visualized by activity staining according to a modified method of Beauchamp and Fridovich (1971). After 20 to 25 min of incubation in the dark at room temperature in staining medium (50 mM potassium phosphate, pH 7.8, containing 1 mM EDTA, 2.8 mM *N,N,N′,N′*-tetramethylethylenediamine, 22 μM riboflavine, and 250 μM nitroblue tetrazolium), gels were exposed to the light until the achromatic band of each SOD isoform became visible. Isoforms were identified by comparison with the previously published Arabidopsis foliar SOD isoform pattern (Kliebenstein et al., 1998)

Gels were scanned using the Bio-Print system. Activities of different forms were evaluated as percentages of activities of SOD in wild-type plants. A pool of leaves from three different plants for each line was taken, and three independent experiments were performed.

Ascorbate, Glutathione, and SA Quantifications

Foliar ascorbate and glutathione were measured as described by Klenell et al. (2005) and Mateo et al. (2006). SA was determined as described by Meuwly and Métraux (1993) from leaves snap frozen in liquid nitrogen. Experiments were performed at least in triplicate at three different time points.

Fixation, Substitution, and Embedding for Transmission Electron Microscopy

Leaves from 8-week-old plants from LL (100 ± 50 μmol m^{-2} s^{-1}) acclimation were treated by fixation, substitution, and embedding according to Börnke et al. (2002) with the following modifications. For primary fixation, 1-mm^2 sections of leaf were kept 4 h at room temperature in 50 mM cacodylate medium (pH 7.2), containing 0.5% (v/v) glutaraldehyde and 2.0% (v/v) formaldehyde, followed by one wash with medium and two washes with distilled water. For the secondary fixation, samples were transferred to a solution of 1% (w/v) OsO_4. After 1 h, samples were washed three times with distilled water. Dehydration of the samples was done stepwise by increasing the concentration of ethanol from 30% to 100% (v/v) for 1 h each. After 1 h of dehydration with propylene oxide, the samples were infiltrated subsequently with Spurr's embedding resin (Plano) as follows: 33% (v/v), 50% (v/v), and 66% (v/v) embedding resin in propylene oxide for 4 h each and then 100% (v/v) embedding resin overnight. Samples were transferred into embedding molds, kept there for 6 h in fresh resin, and polymerized at 70°C for 24 h. For electron microscopy analysis, thin sections with a thickness of approximately 70 nm were cut with a diamond knife and contrasted with a saturated methanolic solution of uranyl acetate and lead citrate. For ultrastructural analysis, a CEM 920A transmission electron microscope (Carl Zeiss) was used at 80 kV.

Supplemental Data

The following materials are available in the online version of this article.

Supplemental Figure S1. Alignment of the predicted amino acid sequences of the *AtGPX* family, phylogenetic tree, and relative transcript levels of different *GPX* genes.

Supplemental Figure S2. Western-blot analysis with antibody raised against cpGPXs.

Supplemental Table S1. Supporting information from microarray data meta-analysis for regulation of the *AtGPX* family in response to different stresses and treatments.

Supplemental Table S2. Relative foliar CAT and APX enzymatic activity and transcript levels in LL-acclimated wild-type, AS-*cpGPX*, and *gpx7* mutant plants.

Received January 13, 2009; accepted April 6, 2009; published April 10, 2009.

LITERATURE CITED

Alscher RG, Erturk N, Heath LS (2002) Role of superoxide dismutases (SODs) in controlling oxidative stress in plants. J Exp Bot **53:** 1331–1341

Alting-Mees MA, Short JM (1989) pBluescript II: gene mapping vectors. Nucleic Acids Res **17:** 9494

Apel K, Hirt H (2004) Reactive oxygen species: metabolism, oxidative stress, and signal transduction. Annu Rev Plant Biol **55:** 373–399

Asada K (1999) The water-water cycle in chloroplasts: scavenging of active oxygens and dissipation of excess photons. Annu Rev Plant Physiol Plant Mol Biol **50:** 601–639

Asada K, Yoshikawa K, Takahashi MA, Maeda Y, Enmanji K (1975)

Superoxide dismutases from a blue-green alga *Plectonema boryanum*. J Biol Chem **250:** 2801–2807

Avery AM, Avery SV (2001) *Saccharomyces cerevisiae* expresses three phospholipid hydroperoxide glutathione peroxidases. J Biol Chem **276:** 33730–33735

Avsian-Kretchmer O, Eshdat Y, Gueta-Dahan Y, Ben-Hayyim G (1999) Regulation of stress-induced phospholipid hydroperoxide glutathione peroxidase expression in *Citrus*. Planta **209:** 469–477

Baker NR (2008) Chlorophyll fluorescence: a probe of photosynthesis in vivo. Annu Rev Plant Biol **59:** 89–113

Ball L, Accotto GP, Bechtold U, Creissen G, Funck D, Jimenez A, Kular B, Leyland N, Mejia-Carranza J, Reynolds H, et al (2004) Evidence for a direct link between glutathione biosynthesis and stress defense gene expression in *Arabidopsis*. Plant Cell **16:** 2448–2462

Bartsch M, Gobbato E, Bednarek P, Debey S, Schultze JL, Bautor J, Parker JE (2006) Salicylic acid-independent ENHANCED DISEASE SUSCEPTIBILITY1 signaling in *Arabidopsis* immunity and cell death is regulated by the monooxygenase FMO1 and the Nudix hydrolase NUDT7. Plant Cell **18:** 1038–1051

Beauchamp C, Fridovich I (1971) Superoxide dismutase: improved assays and an assay applicable to acrylamide gels. Anal Biochem **44:** 276–287

Bechtold U, Karpinski S, Mullineaux PM (2005) The influence of the light environment and photosynthesis on signalling responses in plant-biotrophic pathogen interactions. Plant Cell Environ **28:** 1046–1055

Bevan M (1984) Binary *Agrobacterium* vectors for plant transformation. Nucleic Acids Res **12:** 8711–8721

Börnke F, Hajirezaei M, Heineke D, Melzer M, Herbers K, Sonnewald U (2002) High-level production of the non-cariogenic sucrose isomer palatinose in transgenic tobacco plants strongly impairs development. Planta **214:** 356–364

Bradford M (1976) A rapid and sensitive method for the quantitation of microgram quantities of protein utilizing the principle of protein-dye binding. Anal Biochem **72:** 248–254

Brigelius-Flohé R, Flohé L (2003) Is there a role of glutathione peroxidases in signaling and differentiation? Biofactors **17:** 93–102

Chamnongpol S, Willekens H, Moeder W, Langebartels C, Sandermann H Jr, van Montagu M, Inzé D, van Camp W (1998) Defense activation and enhanced pathogen tolerance induced by H_2O_2 in transgenic tobacco. Proc Natl Acad Sci USA **95:** 5818–5823

Chang CCC, Ball L, Fryer MJ, Baker NR, Karpinski S, Mullineaux PM (2004) Induction of *ASCORBATE PEROXIDASE 2* expression in wounded *Arabidopsis* leaves does not involve known wound-signaling pathways but is associated with changes in photosynthesis. Plant J **38:** 499–511

Chen S, Vaghchhipawala Z, Li W, Asard H, Dickman MB (2004) Tomato phospholipid hydroperoxide glutathione peroxidase inhibits cell death induced by bax and oxidative stresses in yeast and plants. Plant Physiol **135:** 1630–1641

Criqui M, Jamet E, Parmentier Y, Marbach J, Durr A, Fleck J (1992) Isolation and characterization of a plant cDNA showing homology to animal glutathione peroxidases. Plant Mol Biol **18:** 623–627

Depege N, Drevet J, Boyer N (1998) Molecular cloning and characterization of tomato cDNAs encoding glutathione peroxidase-like proteins. Eur J Biochem **253:** 445–451

Dixon RA, Achnine L, Kota P, Liu CJ, Reddy MSS, Wang L (2002) The phenylpropanoid pathway and plant defence: a genomics perspective. Mol Plant Pathol **3:** 371–390

Driscoll SP, Prins A, Olmos E, Kunert KJ, Foyer C (2006) Specification of adaxial and abaxial stomata, epidermal structure and photosynthesis to CO_2 enrichment in maize leaves. J Exp Bot **57:** 381–390

Drotar A, Phelps P, Fall R (1985) Evidence for glutathione peroxidase activities in cultured plant cells. Plant Sci **42:** 35–40

Dutilleul C, Garmier M, Noctor G, Mathieu C, Chétrit P, Foyer C, Paepe RD (2003) Leaf mitochondria modulate whole cell redox homeostasis, set antioxidant capacity, and determine stress resistance through altered signaling and diurnal regulation. Plant Cell **15:** 1212–1226

Ferro M, Salvi D, Brugiere S, Miras S, Kowalski S, Louwagie M, Garin J, Joyard J, Rolland N (2003) Proteomics of the chloroplast envelope membranes from *Arabidopsis thaliana*. Mol Cell Proteomics **2:** 325–345

Foyer C, Noctor G (2000) Oxygen processing in photosynthesis: regulation and signalling. New Phytol **146:** 359–388

Fu LH, Wang XF, Eyal Y, She YM, Donald LJ, Standing KG, Ben-Hayyim G (2002) A selenoprotein in the plant kingdom: mass spectrometry confirms that an opal codon (UGA) encodes selenocysteine in *Chlamydomonas reinhardtii* glutathione peroxidase. J Biol Chem **277:** 25983–25991

Geisler M, Kleczkowski LA, Karpinski S (2006) A universal algorithm for genome-wide *in silico* identification of biologically significant gene promoter putative *cis*-regulatory-elements: identification of new elements for reactive oxygen species and sucrose signaling in *Arabidopsis*. Plant J **45:** 384–398

Genty B, Briantais JM, Baker NR (1989) The relationship between the quantum yield of photosynthetic electron transport and quenching of chlorophyll fluorescence. Biochim Biophys Acta **990:** 87–92

Guerineau F, Mullineaux P (1993) Plant transformation and expression vectors. *In* RRD Croy, ed, Plant Molecular Biology Lab. Bios Scientific Publishers, Oxford, pp 121–147

Guilbault G, Kramer D, Hackley E (1967) A new substrate for fluorometric determination for oxidative enzymes. Anal Chem **39:** 271

Jung BG, Lee KO, Lee SS, Chi YH, Jang HH, Kang SS, Lee K, Lim D, Yoon SC, Yun DJ, et al (2002) A Chinese cabbage cDNA with high sequence identity to phospholipid hydroperoxide glutathione peroxidases encodes a novel isoform of thioredoxin-dependent peroxidase. J Biol Chem **277:** 12572–12578

Karpinska B, Wingsle G, Karpinski S (2000) Antagonistic effects of hydrogen peroxide and glutathione on acclimation to excess excitation energy in *Arabidopsis*. IUBMB Life **50:** 21–26

Karpinski S, Escobar C, Karpinska B, Creissen G, Mullineaux P (1997) Photosynthetic electron transport regulates the expression of cytosolic ascorbate peroxidase genes in *Arabidopsis* during excess light stress. Plant Cell **9:** 627–640

Karpinski S, Gabryś H, Mateo A, Karpinska B, Mullineaux P (2003) Light perception in plant disease defence mechanisms. Curr Opin Plant Biol **6:** 390–396

Karpinski S, Reynolds H, Karpinska B, Wingsle G, Creissen G, Mullineaux P (1999) Systemic signaling and acclimation in response to excess excitation energy in *Arabidopsis*. Science **284:** 654–657

Karpinski S, Wingsle G, Karpinska B, Hallgren JE (1993) Molecular responses to photooxidative stress in *Pinus sylvestris* L. II. Differential expression of CuZn-superoxide dismutases and glutathione reductase. Plant Physiol **103:** 1385–1391

Kiddle G, Pastori GM, Bernard S, Pignocchi C, Antoniw J, Verrier PJ, Foyer CH (2003) Effects of leaf ascorbate content on defense and photosynthesis gene expression in *Arabidopsis thaliana*. Antioxid Redox Signal **5:** 23–32

Klenell M, Morita S, Tiemblo-Olmo M, Mühlenbock P, Karpinski S, Karpinska B (2005) Involvement of the chloroplast signal recognition particle cpSRP43 in acclimation to conditions promoting photooxidative stress in *Arabidopsis*. Plant Cell Physiol **46:** 118–129

Kliebenstein DJ, Monde RA, Last RL (1998) Superoxide dismutase in *Arabidopsis*: an eclectic enzyme family with disparate regulation and protein localization. Plant Physiol **118:** 637–650

Koch E, Slusarenko A (1990) *Arabidopsis* is susceptible to infection by a downy mildew fungus. Plant Cell **2:** 437–445

Lake JA, Woodward FI, Quick WP (2002) Long-distance CO_2 signalling in plants. J Exp Bot **53:** 183–193

Levine A, Tenhaken R, Dixon R, Lamb C (1994) H_2O_2 from the oxidative burst orchestrates the plant hypersensitive disease resistance response. Cell **79:** 583–593

Li WJ, Feng H, Fan JH, Zhang RQ, Zhao NM, Liu JY (2000) Molecular cloning and expression of a phospholipid hydroperoxide glutathione peroxidase homolog in *Oryza sativa*. Biochim Biophys Acta **1493:** 225–230

Mateo A, Funck D, Mühlenbock P, Kular B, Mullineaux PM, Karpinski S (2006) Controlled levels of salicylic acid are required for optimal photosynthesis and redox homeostasis. J Exp Bot **57:** 1795–1807

Mateo A, Mühlenbock P, Rusterucci C, Chang CCC, Miszalski Z, Karpinska B, Parker JE, Mullineaux PM, Karpinski S (2004) Lesion simulating disease 1 is required for acclimation to conditions that promote excess excitation energy. Plant Physiol **136:** 2818–2830

Maxwell K, Johnson GN (2000) Chlorophyll fluorescence: a practical guide. J Exp Bot **51:** 659–668

Métraux JP, Signer H, Ryals J, Ward E, Wyss-Benz M, Gaudin J, Raschdorf K, Schmid E, Blum W, Inverardi B (1990) Increase in salicylic acid at the onset of systemic acquired resistance in cucumber. Science **250:** 1004–1006

Mett VL, Jones WT, Mett VA, Harvey D, Reynolds PHS (2000) Single chain

anti-idiotypic antibody mimics of the phytotoxin dothistromin. Protein Pept Lett **7:** 159–166

Meuwly P, Métraux JP (1993) Ortho-anisic acid as internal standard for the simultaneous quantitation of salicylic acid and its putative biosynthetic precursors in cucumber leaves. Anal Biochem **214:** 500–505

Meyer Y, Reichheld JP, Vignols F (2005) Thioredoxins in *Arabidopsis* and other plants. Photosynth Res **86:** 419–433

Miao Y, Lv D, Wang P, Wang XC, Chen J, Miao C, Song CP (2006) An *Arabidopsis* glutathione peroxidase functions as both a redox transducer and a scavenger in abscisic acid and drought stress responses. Plant Cell **18:** 2749–2766

Milla MAR, Butler E, Huete AR, Wilson CF, Anderson O, Gustafson JP (2002) Expressed sequence tag-based gene expression analysis under aluminum stress in rye. Plant Physiol **130:** 1706–1716

Milla MAR, Maurer A, Huete AR, Gustafson JP (2003) Glutathione peroxidase genes in *Arabidopsis* are ubiquitous and regulated by abiotic stresses through diverse signaling pathways. Plant J **36:** 602–615

Miszalski Z, Ślesak I, Niewiadomska E, Bączek-Kwinta R, Lüttge U, Ratajczak R (1998) Subcellular localization and stress responses of superoxide dismutase isoforms from leaves in the C_3-CAM intermediate halophyte *Mesembryanthemum crystallinum* L. Plant Cell Environ **21:** 169–179

Mittler R (2002) Oxidative stress, antioxidants and stress tolerance. Trends Plant Sci **7:** 405–410

Mittler R, Vanderauwera S, Gollery M, Van Breusegem F (2004) Reactive oxygen gene network of plants. Trends Plant Sci **9:** 490–498

Montillet JL, Chamnongpol S, Rusterucci C, Dat J, van de Cotte B, Agnel JP, Battesti C, Inzé D, Van Breusegem F, Triantaphylides C (2005) Fatty acid hydroperoxides and H_2O_2 in the execution of hypersensitive cell death in tobacco leaves. Plant Physiol **138:** 1516–1526

Mühlenbock P, Plaszczyca M, Plaszczyca M, Mellerowicz E, Karpinski S (2007) Lysigenous aerenchyma formation in *Arabidopsis thaliana* is controlled by *LEASION SIMULATING DISEASE1*. Plant Cell **19:** 3819–3830

Mühlenbock P, Szechyńska-Hebda M, Płaszczyca M, Baudo M, Mullineaux PM, Parker JE, Karpinska B, Karpinski S (2008) Chloroplast signaling and *LESION SIMULATING DISEASE1* regulate crosstalk between light acclimation and immunity in *Arabidopsis*. Plant Cell **20:** 2339–2356

Müller-Moulé P, Golan T, Niyogi KK (2004) Ascorbate-deficient mutants of Arabidopsis grow in high light despite chronic photooxidative stress. Plant Physiol **134:** 1163–1172

Mullineaux PM, Ball L, Escobar C, Karpinska B, Creissen G, Karpinski S (2000) Are diverse signalling pathways integrated in the regulation of *Arabidopsis* antioxidant defence gene expression in response to excess excitation energy? Philos Trans R Soc Lond B Biol Sci **335:** 1531–1540

Mullineaux PM, Karpinski S, Jimenez A, Cleary SP, Robinson C, Creissen GP (1998) Identification of cDNAs encoding plastid -targeted glutathione peroxidase. Plant J **13:** 375–379

Murchie EH, Hubbart S, Peng S, Horton P (2005) Acclimation of photosynthesis to high irradiance in rice: gene expression and interactions with leaf development. J Exp Bot **56:** 449–460

Noh B, Spalding EP (1998) Anion channels and the stimulation of anthocyanin accumulation by blue light in Arabidopsis seedlings. Plant Physiol **116:** 503–509

O'Donnell PJ, Jones JB, Antoine FR, Ciardi J, Klee HJ (2001) Ethylene-dependent salicylic acid regulates an expanded cell death response to a plant pathogen. Plant J **25:** 315–323

Overmyer K, Tuominen H, Kettunen R, Betz C, Langebartels C, Sandermann H Jr, Kangasjärvi J (2000) Ozone-sensitive *Arabidopsis rcd1* mutant reveals opposite roles for ethylene and jasmonate signaling pathways in regulating superoxide-dependent cell death. Plant Cell **12:** 1849–1862

Peltier JB, Ytterberg AJ, Sun Q, vanWijk KJ (2004) New functions of the thylakoid membrane proteome of *Arabidopsis thaliana* revealed by a simple, fast, and versatile fractionation strategy. J Biol Chem **279:** 49367–49383

Rao MV, Paliyath G, Ormrod DP, Murr DP, Watkins CB (1997) Influence of salicylic acid on H_2O_2 production, oxidative stress, and H_2O_2-metabolizing enzymes (salicylic acid-mediated oxidative damage requires H_2O_2). Plant Physiol **115:** 137–149

Rey P, Becuwe N, Barrault MB, Rumeau D, Havaux M, Biteau B, Toledano MB (2007) The Arabidopsis thaliana sulfiredoxin is a plastidic cysteine-sulfinic acid reductase involved in the photooxidative stress response. Plant J **49:** 505–514

Rossel JB, Wilson PB, Hussain D, Woo NS, Gordon MJ, Mewett OP, Howell KA, Whelan J, Kazan K, Pogson BJ (2007) Systemic and intracellular response to photooxidative stress in *Arabidopsis*. Plant Cell **19:** 4091–4110

Roxas V, Smith R Jr, Allen E, Allen R (1997) Overexpression of glutathione S-transferase/glutathione peroxidase enhances the growth of transgenic tobacco seedlings during stress. Nat Biotechnol **15:** 988–991

Shinozaki K, Yamaguchi-Shinozaki K (1997) Gene expression and signal transduction in water-stress response. Plant Physiol **115:** 327–334

Ślesak I, Libik M, Karpinska B, Karpinski S, Miszalski Z (2007) The role of hydrogen peroxide in regulation of plant metabolism and cellular signalling in response to environmental stresses. Acta Biochim Pol **54:** 39–50

Soitamo AJ, Piippo M, Allahverdiyeva Y, Battchikova N, Aro EM (2008) Light has a specific role in modulating Arabidopsis gene expression at low temperature. BMC Plant Biol **8:** 13

Sreenivasulu N, Miranda M, Prakash H, Wobus U, Weschke W (2004) Transcriptome changes in foxtail millet genotypes at high salinity: identification and characterization of a PHGPX gene specifically up-regulated by NaCl in a salt-tolerant line. J Plant Physiol **161:** 467–477

Strawn MA, Marr SK, Inoue K, Inada N, Zubieta C, Wildermuth MC (2007) *Arabidopsis* isochorismate synthase functional in pathogen-induced salicylate biosynthesis exhibits properties consistent with a role in diverse stress responses. J Biol Chem **282:** 5919–5933

Sugimoto M, Sakamoto W (1997) Putative phospholipid hydroperoxide glutathione peroxidase gene from *Arabidopsis thaliana* induced by oxidative stress. Genes Genet Syst **72:** 311–316

Teng S, Keurentjes J, Bentsink L, Koornneef M, Smeekens S (2005) Sucrose-specific induction of anthocyanin biosynthesis in *Arabidopsis* requires the MYB75/PAP1 gene. Plant Physiol **139:** 1840–1852

Tissier AF, Marillonnet S, Klimyuk V, Patel K, Torres MA, Murphy G, Jones JDG (1999) Multiple independent defective suppressor-mutator transposon insertions in *Arabidopsis*: a tool for functional genomics. Plant Cell **11:** 1841–1852

Ursini F, Maiorino M, Brigelius-Flohé R, Aumann KD, Roveri A, Schomburg D, Flohé L (1995) Diversity of glutathione peroxidases. Methods Enzymol **252:** 38–53

Vanderauwera S, Zimmermann P, Rombauts S, Vandenabeele S, Langebartels C, Gruissem W, Inzé D, Van Breusegem F (2005) Genome-wide analysis of hydrogen peroxide-regulated gene expression in *Arabidopsis* reveals a high light-induced transcriptional cluster involved in anthocyanin biosynthesis. Plant Physiol **139:** 806–821

Weigel D, Glazebrook J (2002) Arabidopsis: A Laboratory Manual. Cold Spring Harbor Laboratory Press, Cold Spring Harbor, NY

Wildermuth MC, Dewdney J, Wu GI, Ausubel FM (2001) Isochorismate synthase is required to synthesize salicylic acid for plant defence. Nature **414:** 562–565

Wingsle G, Karpinski S (1996) Differential redox regulation by glutathione of glutathione reductase and CuZn superoxide dismutase gene expression in *Pinus sylvestris* (L.) needles. Planta **198:** 151–157

Winkel BSJ (2004) Metabolic channeling in plants. Annu Rev Plant Biol **55:** 85–107

Zimmermann P, Hirsch-Hoffmann M, Hennig L, Gruissem W (2004) GENEVESTIGATOR: Arabidopsis microarray database and analysis toolbox. Plant Physiol. **136:** 2621–2632

Zybailov B, Rutschow H, Friso G, Rudella A, Emanuelsson O, Sun Q, van Wijk KJ (2008) Sorting signals, N-terminal modifications and abundance of the chloroplast proteome. PLoS One **3:** 1994